J Appl Biotechnol Rep. 2024 June;11(2):1289-1300

Journal of
Applied Biotechnology Reports

doi 10.30491/JABR.2023.398794.1636

Original Article

Molecular Docking and Dynamic Simulation on Investigation and Introduction of some Secondary Metabolites of Medicinal Plants with Antiviral Activity and Effective Vitamins for the Treatment of MPox

Donya Poy [1], **Masoud Tohidfar** [1*]

[1] Department of Cell and Molecular Biology, Faculty of Life Sciences and Biotechnology, Shahid Beheshti University, Tehran, Iran

Corresponding Author: Masoud Tohidfar, PhD, Professor, Department of Cell and Molecular Biology, Faculty of Life Sciences and Biotechnology, Shahid Beheshti University, Tehran, Iran. E-mail: m_tohidfar@sbu.ac.ir

Received May 23, 2023; **Accepted** September 30, 2023; **Online Published** June 20, 2024

Abstract

Introduction: The emergence of the new generation of orthopoxviruses has become as significant concern, including Mpox. With the widespread outbreak of the Mpox virus, various research was conducted on the use of native medicinal plants as medicinal supplements and available vitamins in the field of virus inhibition due to positive therapeutic effects.

Materials and Methods: In this study, we docked and simulated using Molegro Virtual Docker v.6.0 (MVD) software and NAMD program to predict the most probable ligand-to-macromolecule binding combination. First, the sequences were retrieved based on the suitable receptor from the database and we modeled its three-dimensional structure to validate the receptor binding site, by docking three approved drugs, Tecovirimat, Cidofovir, and Brincidofovir as positive controls. Second, 3 candidate plant compounds (Gingerol, Rosmarinic acid, and Gallotannin) and 2 vitamins (vitamin K and vitamin B17) from PubChem were chosen. Eventually, the pharmacokinetic/ADMET properties of these compounds were analyzed.

Results: Our results revealed that the Docking scores of the candidate ligands compared to approve drugs possess higher binding energy with more hydrogen bonds. Based on our findings, the best compounds were chosen for ADMET properties, and these compounds reflected their good pharmacokinetic properties as Mpox inhibitors.

Conclusions: Our results showed that vitamins K and B17 and several plant metabolites, such as gingerol in ginger (Zingiber officinale Roscoe), rosmarinic acid in selfheal (*Prunella vulgaris* L.), rosemary (*Salvia rosmarinus*), and oregano (*Origanum vulgare*), gallotannin in Aleppo oak (*Quercus infectoria*) and Chinese nutgall (*Rhus chinensis*) could possess a good effect in controlling the Mpox.

Keywords: Monkeypox, Plant Metabolites, Vitamins, Molecular Docking and Dynamics

Citation: Poy D, Tohidfar M. Molecular Docking and Dynamic Simulation on Investigation and Introduction of some Secondary Metabolites of Medicinal Plants with Antiviral Activity and Effective Vitamins for the Treatment of MPox. J Appl Biotechnol Rep. 2024;11(2):1289-1300. doi:10.30491/JABR.2023.398794.1636

Introduction

Currently, the world is still grappling with the aftermath of the Coronavirus, with millions of deaths recorded. However, there are whispers of another viral disease known as MPox, which is said to be more frightening than Corona. The first human case of Monkey-Pox (also called MPox by the WHO in 2022)[1] was recorded in the Democratic Republic of Congo in 1970.[2] Since then, MPox has been reported in humans in other Central and West African countries. In the 1970s, smallpox spread throughout the world, but with the discovery of the smallpox vaccine, it was eradicated, and people were vaccinated in 1980.[3,4] Following the eradication of smallpox through vaccination, the world stopped vaccinating against the disease. This created an opportunity for the spread of common pathogenic viruses between humans and animals from the Orthopoxvirus family, including MPox, cowpox, and camel-pox, which have adapted mutations. However, MPox is still endemic in sub-Saharan Africa and has spread to non-native European, American, and Asian countries, including Great Britain, Germany, France, Canada, Australia, Italy, Belgium, Spain, Holland, Portugal, Sweden, America, India, and Thailand.[5,6] Initially, the primary source of transmission for MPox was believed to be through contact with infected animals in nature (zoonotic) in endemic areas of Africa. However, in 2018, several cases of human-to-human transmission were confirmed in the UK and other countries.[7-9]

Both smallpox (Variola virus) and MPox (MPox virus) belong to the Orthopoxvirus family of double-stranded DNA viruses, with slight differences in their structures.[10] Symptoms of MPox are similar to smallpox and include fever, headache, back pain, skin rash, and flu-like symptoms.[2] Various diagnostic methods are used to detect

MPox, including PCR, culture, and immunohistochemistry such as ELISA or electron microscopy, depending on test availability.[11,12] According to a 2019 report by Erez et al., the viral particles detected have a size of 281 ± 18 nm × 220 ± 17 nm (n = 24).[12] Despite the clinical similarity of smallpox and Mpox, Mpox is much more worrisome and causes more deaths.[13] On the other hand, bioinformatic studies, also confirm the genetic sequence similarities between different types of Orthopoxviruses, such as cowpox viruses, Buffalopox viruses, Akhmeta viruses, and Alaskapox viruses, especially in their conserved regions and domain function.

Today, there is preliminary research, and we are faced with a widespread outbreak of the MPox virus worldwide. Currently, several experimental drugs used to treat smallpox, such as Tecovirimat, which has been approved by the US FDA, are also used to treat MPox. Additionally, drugs such as Cidofovir or Brincidofovir have been used to treat MPox and have shown some effectiveness.[11] Currently, there is a lack of extensive *in-silico* studies on the effectiveness of other drugs in treating MPox outside of experimental models. Conducting such studies could increase our knowledge of how to treat MPox.

One resource that is available to the public in all countries is the use of native medicinal plants. In addition to their independent use, medicinal plants can also be used as a supplement to approved drugs.[14,15] Many studies have shown that functional compounds derived from medicinal plants, called secondary metabolites, proteins, and peptides have proven to be effective in treating various chronic diseases, with activities such as anti-cancer, antibacterial, antifungal, anti-inflammatory, anti-allergy, and even antiviral by membrane permeability, virus replication, and cellular function.[16,17] Drugs and herbal compounds have antiviral activities that primarily involve inhibiting virus entry through surface proteins, and the synthesis and replication of the virus genome, which includes DNA or RNA. Therefore, for the design of effective antiviral drugs, it is crucial to pay attention to the structure of the virus and its replication cycle.[14,18] On the other hand, it has been proven that trace elements and vitamins have been shown to have a significant impact on enhancing immune system functioning. A wide range of minerals and vitamins are involved in metabolic machinery that is responsible for biosynthesis and energy generation.[19,20] According to the literature, some viral diseases, such as Coronavirus, may benefit from vitamin treatment.[21] In acute COVID-19, disease severity was independently associated with vitamin K and vitamin D deficiency, suggesting that these two vitamins may work together synergistically.[22] Hepatitis C infection increases oxidative stress and decreases group B vitamin levels in the bloodstream, and food supplements and vitamin B consumption can be beneficial in preventing further damage and the spread of the disease.[23] Vitamin B17 (amygdalin) has anti-cancer properties, and its deficiency has been hypothesized to cause cancer.[24,25] It has traditionally been used to treat asthma, bronchitis, diabetes, and vaginal infections.[26].

This study aims to investigate various types of antiviral secondary metabolites using *in-silico* methods to inhibit MPox virus entry through surface proteins in comparison with existing drugs. Considering the global availability of medicinal plants and vitamins as necessary supplements, these computational studies to determine the antiviral, antibacterial, and antifungal properties can open new doors for experts to conduct further experimental studies.

Materials and Methods

Molecular Docking

This study examined the antiviral properties of 61 plant metabolites (provided in Supplementary Table 1), as well as 10 vitamins, based on both traditional claims and new research. The 2D and 3D structures of these metabolites were obtained from the PubChem chemical database (https://pubchem.ncbi.nlm.nih.gov).[27] To prepare the ligands for docking and molecular dynamics (MD) studies, the 2D structures were converted into 3D structures using ChemDraw v. Ultra 7.0 software. The energy minimization process was performed using the same software through the MM2 force field. In addition, the 3D structures of standard and approved drugs for MPox, including Tecovirimat, Cidofovir, and Brincidofovir, were obtained from the drug bank (https://go.drugbank.com)[28] and stored as controls for comparison. The docking scores of the antiviral metabolites were then compared with those of the standard drugs to assess their potential effectiveness as antiviral agents.

The primary objective of this study was to inhibit the surface protein of the MPox virus. To achieve this goal, we searched the NCBI database for "MPox virus cell surface binding protein" and selected the amino acid FASTA sequence with accession number Q8V4Y0 from the E8L gene (isolated from the Zaire-96-I-16 strain of MPox virus)[29] However, the 3D structure of this amino acid sequence was not available in the protein data bank. To address this, we used the I-TASSER server,[30] a protein structure prediction tool that also provides structure-based function annotation, to model and fold the protein and create its 3D structure (https://zhanggroup.org/I-TASSER) (Figure 1). Among the predicted models, we saved the one with the highest C-score in PDB file format. With the E8L protein now available in 3D structure, we considered it as the receptor in this study and made preliminary preparations for docking. These preparations included the addition of polar hydrogens and charges, as well as the minimization of structural energy.

We performed docking studies of our candidate ligands and receptor using Molegro Virtual Docker v.6.0 (MVD) software, which is a fast and flexible docking program.

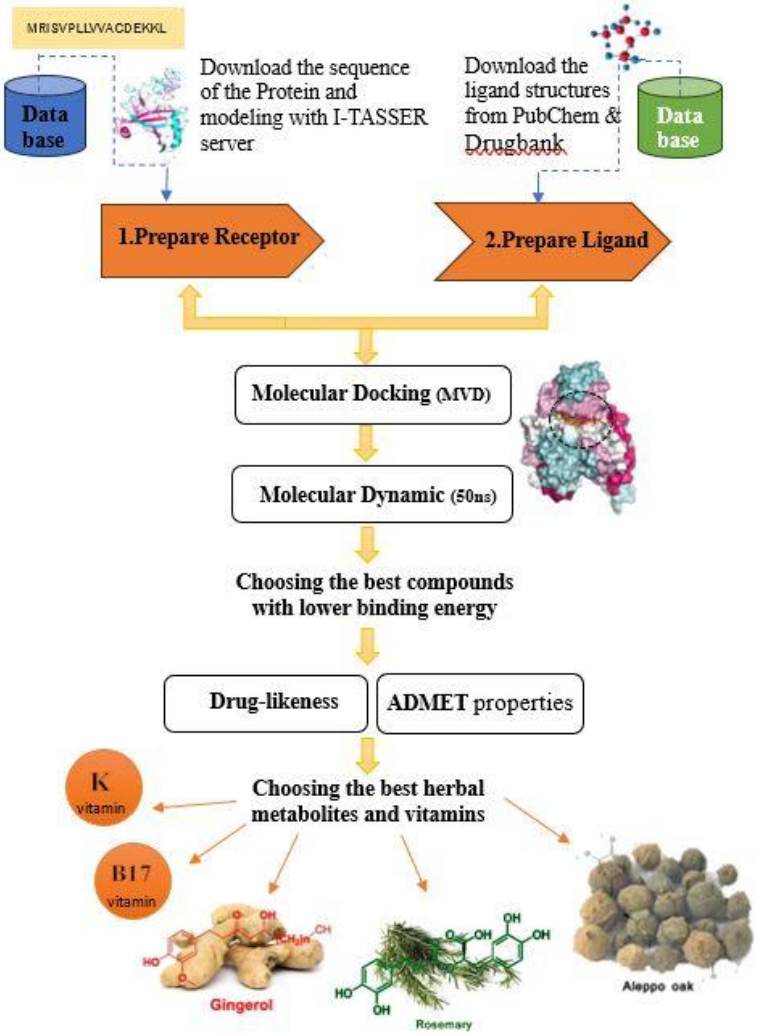

Figure 1. A Generally Overview of this Study's Method by Presenting a Flowchart.

MolDock software, which is based on a new heuristic search algorithm, was used to predict the most probable ligand-to-macromolecule binding combination by combining differential evolution with a cavity prediction algorithm, with a high confidence coefficient.[31]

Before docking, we identified the possible binding sites of the ligand to the receptor in the form of cubic holes. Using data obtained from the Coach server, we identified approximately 16 residues, including Asn158, Tyr265, Tyr155, Ile281, Ile26, Ile279, Val282, Phe283, Ile290, Leu291, Asp25, His27, Tyr28, Asn29, Leu24, and Asp157 as the binding sites (active site) of the E8L receptor. These results were confirmed by docking three approved drugs, Tecovirimat, Cidofovir, and Brincidofovir, to determine the receptor binding site. As shown in Figure 1, all three drugs were placed in a junction box. In the first step, we entered the protein as the receptor into the MVD software to reconstruct the residues with structural errors, and the ligands were prepared using the default settings. We selected the MolDock SE algorithm for the scoring function to perform the docking process. The MVD software determined five different binding sites (cavities) of the E8L protein as the receptor. We selected the MolDock SE algorithm as the scoring function for the docking process. In addition, we chose a spherical region of radius 23 Å, with structural coordinate values X = 62.96, Y = 64.64, and Z = 62.02, to define the binding site of ligands. To ignore atoms that are far away from the binding site, we chose the ignore-distant-atoms option, and hydrogen bonding between potential donors and acceptors was investigated. We calculated the ligand-receptor (protein) interaction energy, which provided the docking scores. Better binding affinity was identified with more negative scores.[32] To rank the inhibitor poses according to experimental docking studies, we used the MolDock re-rank scores for all ligands and drugs, selecting the better-chosen poses. The re-ranking scoring functions can calculate chemical properties using molecular models that were created and predicted. Re-rank scores are outstanding in ranking different poses of a particular ligand. Therefore, it is recommended that virtual

screening results are ranked using the re-rank score.[33]

Molecular Dynamics (MD) Simulations

We performed molecular dynamics simulations for the ligands with minimal binding energy (stronger binding) using the NAMD program (model: Git_2022_05_28), and the files were generated with Visual Molecular Dynamics (VMD).[34,35] The protein was solved with a TIP3P water box and CHARMM 22 parameter files, with phi and psi cross-term map correction, applied to force fields for proteins whose chemical structures are similar.[36,37] To minimize and balance the protein in the water box, we assumed force field parameters without scaling of 1.0 Å, and a cutoff of Coulomb forces with a switching function that starts at 12 Å, goes to zero at a distance of 10 Å, and ends at 13.5 Å with a margin of 3.0 Å. All atoms, including hydrogen atoms, were explicitly represented. We generated the coordinates of the hydrogen atoms of the protein using the VMD Tk-Console salvation command.[34] In addition, we used integrator parameters of 2 fs/step for all inflexible bonds, and nonbonded frequencies were set to 1 Å, with complete electrostatic reviews for 2 Å. We executed periodic boundary conditions with grid dimensions of 1.5 Å for electrostatic interactions of the protein via the particle mesh Ewald technique. The 3D structure of the E8L protein receptor includes 304 amino acids, and the number of water molecules inside the simulation box is 4500.

To remove bad water constraints, we minimized the preliminary energy of the protein through 5,000 stages of Powell's algorithm at a constant temperature of 310 K. The simulation was done with Langevin dynamics to examine the kinetic energy, temperature, and/or pressure of the system without a binding pocket, as none of the desired parameters should change the protein structure during ligand dissociation. After performing the preliminary simulations of the protein, we selected the protein-ligand complexes and used the SwissParam server for parameterization.[37,38] Once the ligands were parametrized, we embedded them in the protein and stored them as a protein-ligand complex by VMD, with the binding pocket residues immersed in the center of the box of water molecules.[37,39]

Ultimately, we balanced the simulation with a solvated protein-ligand complex with 5,000 minimization steps and 25,000,000 runs for 50 ns. At the end of the simulation, we analyzed the results by calculating the RMSD, root mean square fluctuation (RMSF) trajectories, hydrogen bond distances, and the radius of gyration (Rg), using VMD and generated the graphs using the Matplotlib 3.6.3 library of Python.

Study of Pharmacokinetic Indicators

Computational technology has become a vital tool in drug candidate recognition as it reduces the need for experimental drug trials and increases the probability of success. To investigate the pharmacokinetic/ADMET properties of these compounds and generate predictive models of central ADMET properties using graph-based signatures, we used the pkCSM online web server (http://structure.bioc.cam.ac.uk/pkcsm) for drug discovery. We also checked the pharmacological similarity between these compounds using another online server tool called SWISSADME (http://www.swissadme.ch/index.php). In the early stages of drug discovery, we used Lipinski's rule of five (RO5)[40,41] to guide the selection of compounds.

Results

Molecular Docking

We initially selected E8L protein as receptor and 71 compounds [61 plant metabolites as well as 10 vitamins (provided as a supplementary Table 1)] as ligands based on the literature review on the antiviral properties of medicinal plants and some vitamins. After docking, we ignored ligands with higher MolDock scores than approved drugs. Therefore, we selected 28 compounds, including medicinal plant compounds and vitamins, for the next steps. Using the MVD software, we categorized all remaining compounds by their binding energy. Finally, we selected five compounds, including three medicinal plant compounds and two vitamins, with higher MolDock scores (more negative), fewer side effects, more appropriate dosage, and more accessibility to people, for the molecular simulation stage (Table 1 & 2).

Table 1. *In-silico* Docking Analysis of Approved Drug Ranking based on MolDock Score

No	Existing Drug	PubChem Cod.	MolDock Score (Energy kcal/mol)	Re-rank Score (kcal/mol)	H-Bond Energy (kcal/mol)
1	Tecovirimat	16124688	-98/73	-80/98	-1/4273
2	Cidofovir	60613	-118/57	-91/21	-13/2102
3	Brincidofovir	483477	-144/74	-102/63	-6/30133

Table 2. *In-silico* Docking Analysis of Candidate Compounds Ranking based on MolDock Score

No	Ligands	PubChem Cod.	MolDock Score (Energy kcal/mol)	Re-rank Score (kcal/mol)	H-Bond Energy (kcal/mol)
1	Gingerol	442793	-133/34	-100/85	-11/0256
2	Rosmarinic acid	5281792	-156/51	-122/37	-16/1418
3	Gallotannin	452707	-191/19	-125/89	-16/8782
4	Vitamin K	5280483	-130/34	-99/13	-2/0700
5	Vitamin B17	656516	-161/60	-118/34	-14/9936

Table 3. Comparative Evaluation of the Active Sites and other Binding Site Residues for Receptor-Ligand Complexed

No.	Receptor–Ligand interactions		H-Bond* and Steric interaction
1	E8L receptor complexed with approved drugs	Tecovirimat	**Ile281***, Asp157, Phe276, Ala280, His27, Asp25, Ile26, Val284, Leu24, Val282, Ile279, Phe283, Leu164, Thr23
		Cidofovir	**Asp25***, Phe276, **Asn29***, **Tyr28***, His27, **Asp157***, Ile281, Phe283, **Leu24*,** Ala280, Leu164, Val284, Thr23, Val282, Ile279, Leu160, **Ile26***
		Brincidofovir	**Asn158***, **Tyr265***, Tyr155, Val153, Tyr130, **Asp157*,** Asn29, Ile281, His27, Ile26, Val284, Leu164, Phe283, Thr 23, Ile 290, Leu291, Val 282, Leu160, Phe276, Ile279, Ala280, Leu24, **Asp25***
2	E8L receptor complexed with Gingerol		Leu164, Thr23, Val284, Leu160, Asp25, **Ile26***, Phe283, Val282, **Leu24***, Ile279, Ala280, Ile281, Phe276, **Tyr28***, **Asp157***, **Asn29***, His27
3	E8L receptor complexed with Rosmarinic acid		**Leu24***, **Thr23***, Phe283, Leu160, Ile279, **Asp25***, Ala280, Phe276, **Asn29***, **Asp157***, Ile281, Tyr28*, His27, Val282, **Ile26***, Val284, Leu164
4	E8L receptor complexed with Gallotannin		**Tyr51***, His27, Asn29, **Val282***, Phe283, Ile281, **Leu24***, Thr23, Ile279, **Ile26***, Asp25, Leu164, **Asn158***, **Tyr265***, Asp157, Asn273, Phe276, Tyr155
5	E8L receptor complexed with Vitamin K		Ile290, Val282, His27, Ile281, Asn29, Tyr28, Asp157, **Ile26***, Asp25, Leu160, Phe276, Phe283, Ile279, Leu24, Ala280
6	E8L receptor complexed with Vitamin B17		**Asp25***, Val28, Phe283, Val284, Thr23, Ile279, Leu164, **Leu24***, Leu160, Phe276, **Ile26***, **Asp157***, **Asn29***, **Tyr28***, His27, Glu271, Leu291, Gly272, Ile281

Bold and asterisked residues are involved in forming hydrogen bonds in the ligand-receptor complex

We found that the binding patterns of candidate compounds are similar to existing approved drugs based on the *in-silico* docking of three approved drugs with the MVD inspector tool. Hydrogen bonding plays a crucial role in the stability of structures and functions, and the type of ligand-receptor active site interaction can be best described by analyzing hydrogen bonds. Using the Coach server, we identified approximately 16 residues, including Asn158, Tyr265, Tyr155, Ile281, Ile26, Ile279, Val282, Phe283, Ile290, Leu291, Asp25, His27, Tyr28, Asn29, Leu24, Asp157, as binding sites (active site) of the receptor. These results were confirmed by blind docking with three approved drugs (Tecovirimat, Cidofovir, and Brincidofovir).

Table 3 shows that some amino acids of the ligands established more stable interactions in the receptor's active site by forming more hydrogen bonds. We validated the hydrogen bonds and steric interaction of candidate ligands in the receptor active site by investigating the connections of the drug-receptor complex. As depicted in Figure 2, these interactions were consistent with the drug-receptor complexes.

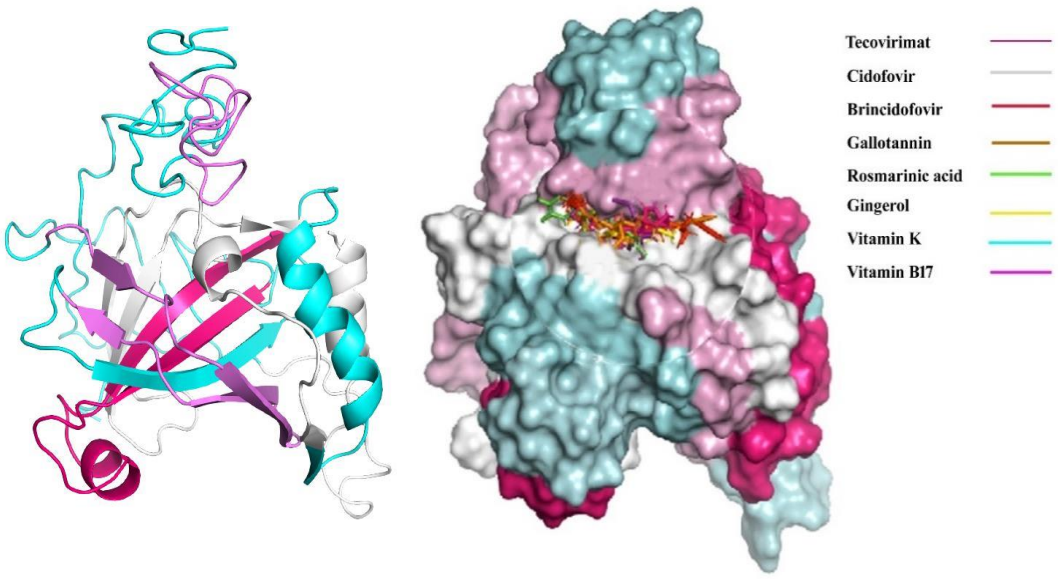

Figure 2. 3D Visualizations of Approved Drugs and Candidate Ligands in the Active Site of E8L Receptor (protein modeled by I-Tasser) with Pymol.

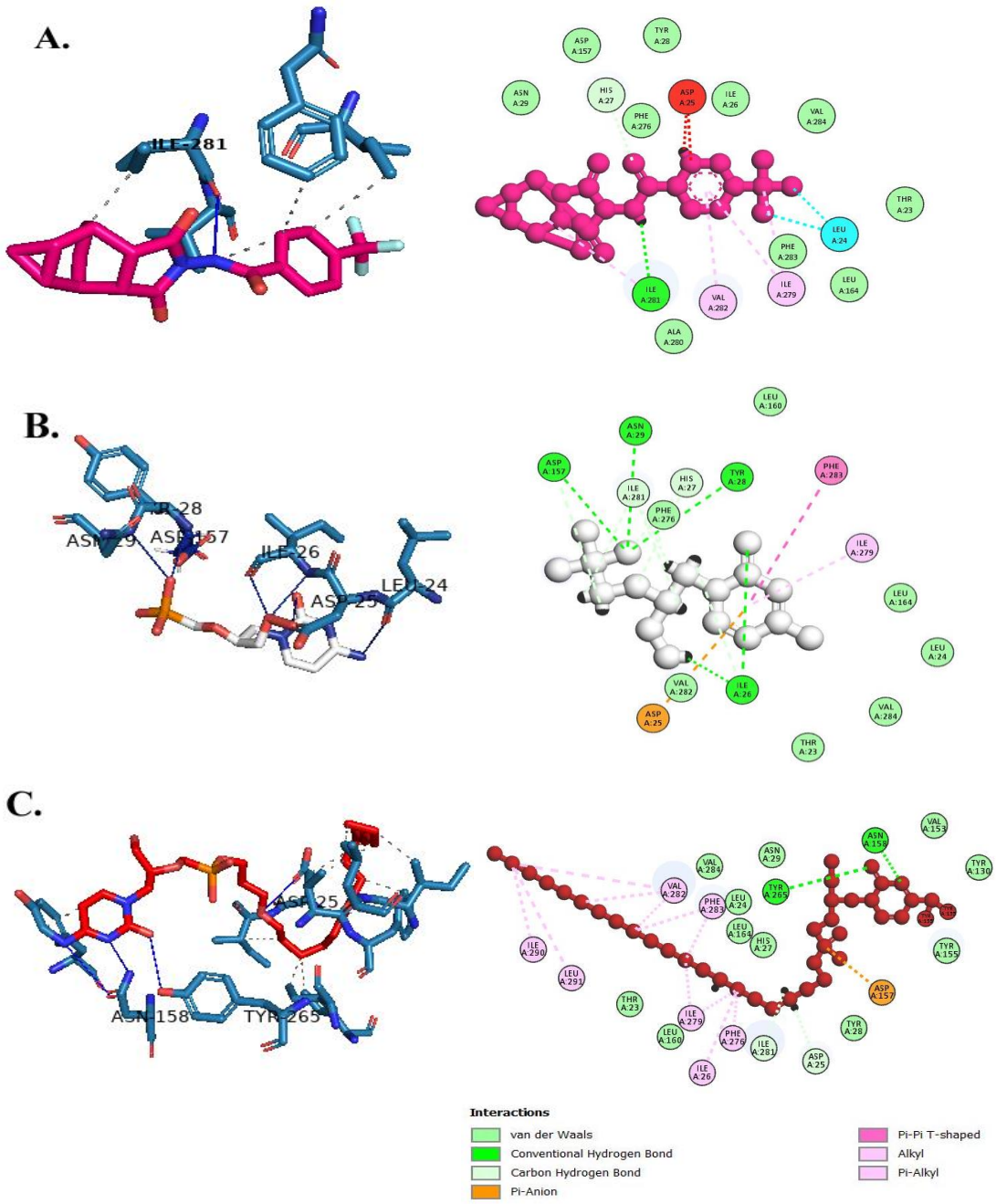

Figure 3. 3D and 2D Molecular Interactions of Hydrogen and Steric Bonds with Functional Residues of the Drug-Receptor Complex by Protein-Ligand Interaction Profiler (PLIP) Server and BIOVIA Discovery Studio 2021. A) Tecovirimat (pink) with one hydrogen bond; B) Cidofovir (white) with six hydrogen bonds; C) Brincidofovir (red) with four hydrogen bonds. (Notes: Blue lines in 3D and dark green lines in 2D figures indicate hydrogen bonds, dotted lines indicate steric bonds, and the type and number of involved residues are fully described in Table 3.)

Tecovirimat, Cidofovir, and Brincidofovir, the three approved drugs used as controls, had binding energies of -98/73 (Re-rank: -80/98), -118/57 (Re-rank: -91/21), and -144/74 (Re-rank: -102/63) (kcal/mol), respectively, with one, six, and four hydrogen bonds. Based on these results, Brincidofovir had higher binding energy than Cidofovir despite having a lower number of hydrogen bonds. It can be argued that although Brincidofovir does not form an extensive network of hydrogen bonds and steric interactions in the binding cavity, it creates more effective hydrogen bonds than Cidofovir (Table 1, 3, & Figure 3).

The candidate ligands in this study also showed interesting results in terms of their binding patterns with the receptor. Gingerol, with five hydrogen bonds, had binding energy of -133.34 (Re-rank: -100/85) kcal/mol, while Rosmarinic acid and Gallotannin, with six hydrogen bonds, had binding energies of -156.51 (Re-rank: -122/37) and -191.19 (Re-rank: -125/89) kcal/mol, respectively.

The results showed that among the vitamins, vitamin K and vitamin B17 had the highest binding energies with the receptor. Vitamin K formed one hydrogen bond with the receptor and had a binding energy of -130.34 (Re-rank: -99/13) (kcal/mol),

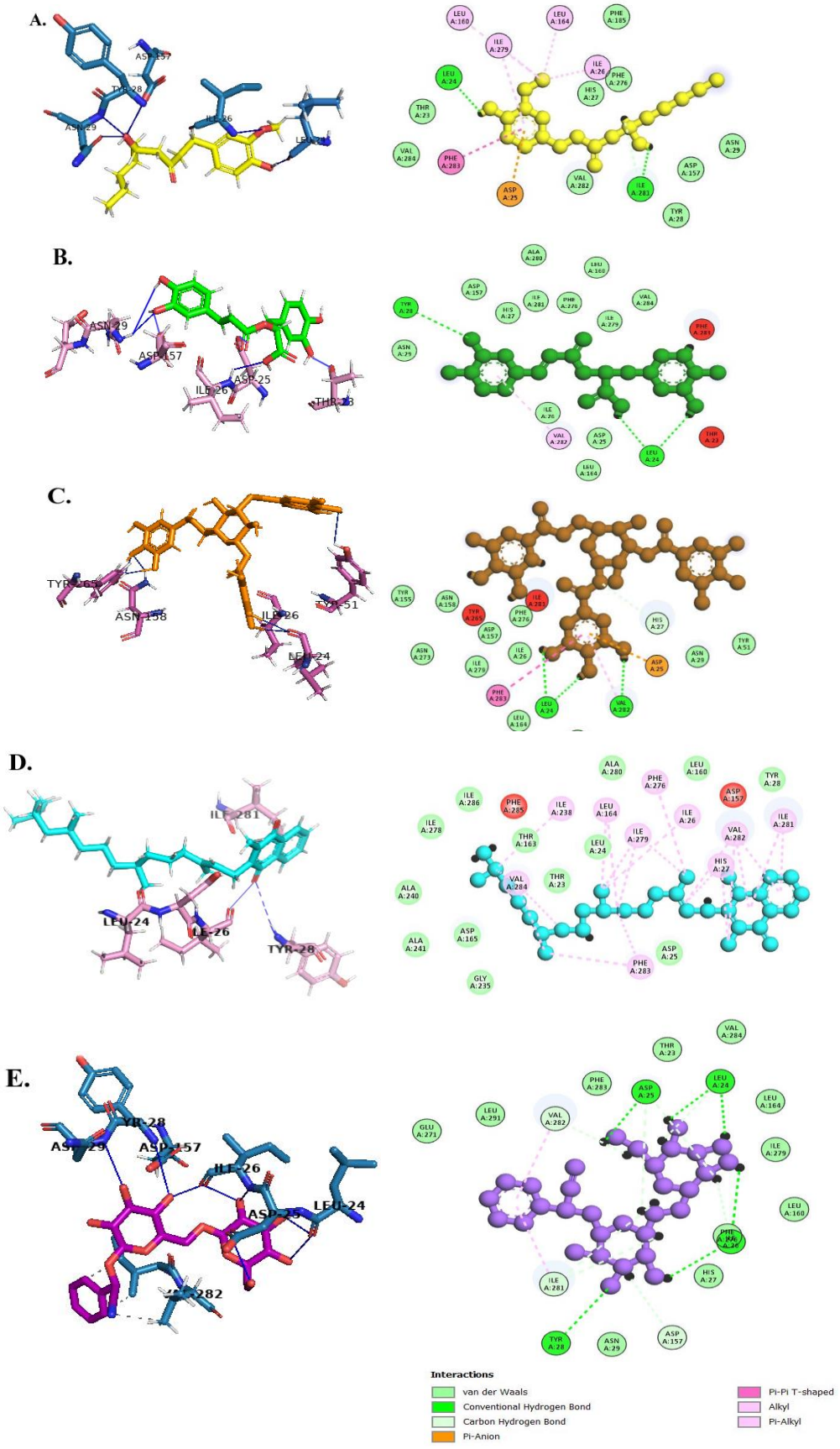

Figure 4. 3D and 2D Molecular Interaction of Hydrogen and Steric bonds with Functional Residues of the Ligand-Receptor Complex by Protein-Ligand Interaction Profiler (PLIP) Server and BIOVIA Discovery Studio 2021. A) Gingerol (yellow) with five hydrogen-bond; B) Rosmarinic acid (green) with six hydrogen-bond; C) Gallotannin (brown) with six hydrogen-bond; D) Vitamin K (cyan) with one hydrogen-bond; E) Vitamin B17 (purple) with eight hydrogen-bond. (Notes: Blue lines in 3D and dark green lines in 2D figures show hydrogen bonds, and dotted lines show steric bonds, the type, and the number of involved residues are reviewed in Table 3 completely).

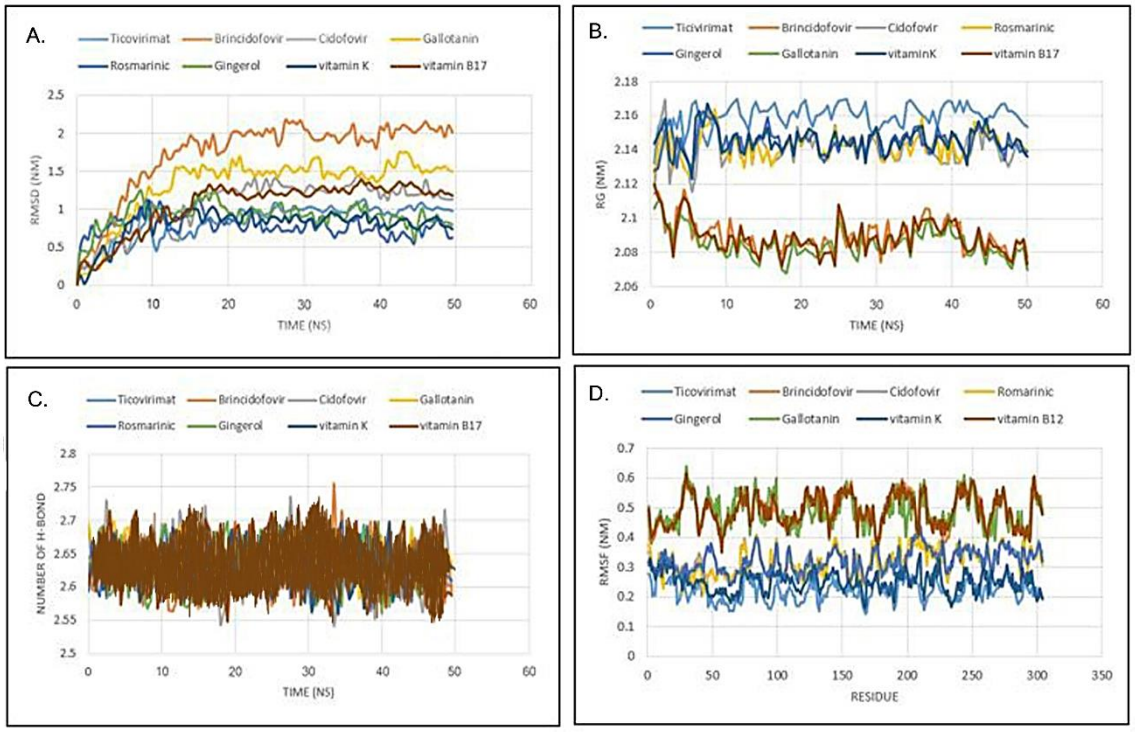

Figure 5. Investigation of 50 ns Performance of Molecular Dynamics Simulations. A) Plot of RMSD vs. Time for All Control and Candidate Complexes; B) Plot of Radius of Gyration (Rg) for All Control and Candidate Complexes; C) Evaluation of Ligand-Receptor Interaction by Number of Hydrogen Bonds as a Function of Time; D) Plot of Root Mean Square Fluctuation (RMSF) for the Complexes Obtained During 50 ns MD Simulations.

while vitamin B17 formed eight hydrogen bonds and had a binding energy of -161.60 (Re-rank: -118/34) (kcal/mol) (Table 2, 3, & Figure 4)

Molecular Dynamics (MD) Simulations

We calculated the root mean square deviation (RMSD) of the atomic positions of the drug-receptor complexes as inhibitors of viral protein to examine conformational variations. The stability of the ligands and protein atoms was analyzed by calculating the root mean square deviation (RMSD) as a function of simulation time (final molecular dynamics run of 50 ns), and the results are presented in Figure 5 (A). The RMSD values for each complex were determined for a box with structural coordinates of x = 51, y = 55, and z = 62, and the results showed that the complexes achieved stability after 20 ns. Among the three drugs investigated, Tecovirimat exhibited the highest stability, followed by Cidofovir and Brincidofovir. In addition, the stability patterns of five candidate ligands, namely Rosmarinic acid, Gingerol, Vitamin K, Vitamin B17, and Gallotannin, were compared to those of the drugs. The results indicated that all five ligands were more stable than the drugs (Figure 5A). The overall stability of the complexes was evaluated by analyzing the radius of gyration (Rg) plots, which are presented in Figure 5B. The results showed that after 20 ns, the Rg plots did not exhibit significant changes during the simulation.

Table 4. The ADMET Properties of the Approved Drugs

No.	Approved Drug	Molecular weight (g/mol) (≤500 Da)	Num. H-bond acceptors (≤10)	Num. H-bond donors (≤5)	MLOGP (<5)	No. of Lipinski's violations	Bioavailability Score	Druglikeness
1	Tecovirimat	376.33	6	1	3.91	0	0.55	YES
2	Cidofovir	279.19	7	4	-2.25	0	0.11	YES
3	Brincidofovir	561.69	8	3	1.23	1	0.55	YES

Table 5. The Predicted Drug-Likeness Properties of the Approved Drugs

DRUG	Absorption HIA	Distribution BBB permeability (Log BB)	CNS Perm. (Log PS)	Metabolism Substrate Inhibitors CYP					EXCRETION Total Clearance	TOXICITY AMES Toxicity	LD50
				2D6	3A4	1A2	2C19	2C9			
1	92.812	0.41	-2/339	NO	YES	NO	YES	NO	-0/434	NO	2/743
2	66/822	-1/288	-3/779	NO	NO	NO	NO	NO	0/277	NO	1/74
3	70/031	-2/106	-4/272	NO	YES	NO	NO	NO	0/924	NO	2/531

Table 6. The ADMET Properties of the Candidate Ligands

Molecules	Plant Metabolits	Molecular weight (g/mol) (≤500 Da)	Num. Hbond acceptors (≤10)	Num. Hbond donors (≤5)	MLOGP (<5)	No. of Lipinski's violations	Bioavailability Score	Druglikeness
14	Gingerol	294.39	4	2	2.14	0	0.55	YES
19	Rosmarinic acid	360.31	8	5	0.90	0	0.56	YES
23	Gallotannin	636.47	18	11	-2.42	4	0/17	NO
28	Vitamin K	450.70	2	0	5.64	1	0.55	YES
29	Vitamin B17	457.43	12	7	-3.58	2	0.17	NO

Drug Likeness and In-silico ADMET Prediction Analysis

In evaluating the good permeability of drug molecules, various indicators, such as Log P, TPSA, MW, HBA, and HBD, are typically calculated to assess their hydrophobicity properties. The SWISSADME and pkCSM servers were used to calculate the pharmacokinetic parameters ADMET and drug-likeness of all three drugs, and the results are presented in Tables 4 & 5. These parameters confirmed the viability of the drugs and demonstrated that all three compounds satisfied the derivatives of the Lipinski rule (MW ≤500 Da, LogP <5, nHBD ≤5, nHBA ≤10, and TPSA <140 Å).

Notably, although Brincidofovir exhibits a molecular weight greater than 500, which plays a crucial role in a drug's oral bioavailability, the 500 Da cut-off mark does not seriously categorize compounds as having poor or good oral bioavailability. Brincidofovir is an oral antiviral drug used in the treatment of human smallpox infections, despite its higher molecular weight. However, as a general rule, most compounds that do not meet two or more parameters of the Lipinski rules can be considered non-bioavailable when taken orally.[46]

Table 5 shows that all three drugs exhibit good human intestinal absorption percentages, with minimum recommended values of 30%. The recommended values for blood-brain barrier (BBB) and central nervous system permeabilities are >0.3 to <-1 Log BB and >-2 to <-3 Log PS, respectively. In the human body, the enzymatic metabolism of drugs is measured with cytochrome P450, which plays a key role in drug metabolism. Among the CYP family indicators, 3A4 is significant because most compounds are reported to be its substrates and inhibitors.

Total clearance is another important indicator that explains the relationship between the rate of exclusion of the drug and its concentration in the body. It is important to note that elimination and clearance have different meanings. While elimination explains the rate of waste or damage (mg/h, amount per time), clearance defines units of flow (L/h, volume per time). Therefore, the elimination of a drug is a linear function of the drug concentration when the clearance is constant.[42] Based on the provided information, it is noteworthy that Brincidofovir, although an oral drug, does not fall within the approved range for BBB (Log BB >-1) and central nervous system permeability (Log PS>-3).

Following the examination of the ligands' affinity to the MPox virus protein during docking and molecular simulation, their drug-likeness properties and ADMET were assessed. Table 6 shows that all ligands, except Gallotannin, exhibit suitable molecular weights. However, as noted in previous sections, a molecular weight >500 does not necessarily classify a compound as having poor oral bioavailability, as exemplified by Brincidofovir.

All compounds were found to be fat-soluble (LogP<5), which is important for drug absorption, transport, and distribution. Notably, even though vitamin K exhibited a LogP value of 5.64, it is still considered fat-soluble. According to Table 6, Gallotannin and Vitamin B17 violated more than two of Lipinski's rules and are not classified as drugs, although Vitamin B17 is commercially available in pharmacies. The data in Table 7 demonstrate that, despite the non-toxicity of all compounds, Gallotannin and Vitamin B17 exhibit inadequate intestinal absorption (minimum recommended amounts of 30%). The central nervous system permeability (LogPS) indicator should be >-2 to <-3, which is -5/183 for Gallotannin. However, all compounds, except Gingerol and Vitamin B17, demonstrated acceptable total clearance.

Table 7. The Predicted Drug-Likeness Properties of the Candidate Ligands

molecules	Absorption HIA (%)	Distribution BBB permeabiliy (Log BB)	CNS Perm.(Log PS)	Metabolism Substrate Inhibitors CYP					Excretion Total Clearance	Toxicity AMES Toxicity	LD50
				2D6	3A4	1A2	2C19	2C9			
Gin	92/416	-0/727	-2/788	NO	NO	YES	YES	YES	1/339	NO	1/958
Ros	32/516	-1/378	-3/347	NO	NO	NO	NO	NO	0/25	NO	2/811
Gal	0/523	-3/569	-5/183	NO	NO	NO	NO	NO	0/417	NO	2/483
K	96/834	-0/281	-1/108	NO	YES	YES	YES	YES	0/877	NO	1/72
B17	26/722	-1/236	-3/857	NO	NO	NO	NO	NO	1/12	NO	2/223

Discussion

Several studies have demonstrated the efficacy of certain drugs against orthopoxviruses, including the MPox virus. For instance, Desai et al. (2022) reported that tecovirimat was well-tolerated with minimal adverse effects in patients with MPox infection during clinical trials and displayed a

favorable safety profile. Brincidofovir, a nucleotide analog that is FDA-approved, has also shown promising results against MPox in rodent models.[43,44] Cidofovir has been demonstrated to prevent lesions in non-human primates up to 48 hours after exposure to MPox and infection.[45] According to a 2022 report by Siegrist et al., all three antiviral drugs, cidofovir, brincidofovir, and tecovirimat, showed good activity against MPox, with tecovirimat and brincidofovir presenting more promising tolerability profiles for treatment options. However, more clinical trials are needed to gain a better understanding of their efficacy and safety profiles.[45] The results showed that the binding patterns and hydrogen bond connections of the ligand-receptor complex for each candidate compound, with Gingerol showing similarities to Cidofovir, Gallotannin showing similarities to Brincidofovir, and Rosmarinic acid showing similarities to both Cidofovir and Brincidofovir. Although Tecovirimat and vitamin K formed only one hydrogen bond with the receptor, vitamin K had a higher binding energy, indicating that it may bind with a more effective residue. While Vitamin B17 had a higher binding energy than Cidofovir, its hydrogen bond pattern was similar to Cidofovir and Brincidofovir.

In the investigations carried out in the molecular dynamics section two distinct patterns were observed: one for Brincidofovir, Gallotannin, and Vitamin B17, and another for Cidofovir, Rosmarinic acid, Gingerol, Vitamin K, and Tecovirimat. The compression of the systems remained relatively stable during the simulation, with only minor changes. Interestingly, the Rg pattern of Gallotannin and Vitamin B17 was found to be compatible with that of Brincidofovir, while Rosmarinic acid, Gingerol, and Vitamin K exhibited a similar pattern to Cidofovir. Tecovirimat showed a larger Rg than the other compounds tested. Since hydrogen bonds are crucial for the stability of complexes, analyzing the hydrogen bond plot is essential to evaluate their stability during molecular simulation. Figure 5C presents the hydrogen bond plots, which demonstrated a single and similar pattern for all the complexes during the simulation. As expected from the molecular docking results, the hydrogen bond pattern in Brincidofovir and Cidofovir exhibited more vigorous changes during the simulation than in Tecovirimat. Additionally, all ligands, except Vitamin K, demonstrated an increase in hydrogen bonds during the simulation, indicating better stability than the drugs. To assess the vibration of each residue during the simulation, the root mean square fluctuation (RMSF) plot was generated and analyzed. The results revealed three distinct patterns of behavior based on the approved drugs. Specifically, Gallotannin and Vitamin B17 exhibited similar RMSF patterns with Brincidofovir and Rosmarinic acid, while Gingerol exhibited a similar pattern with Cidofovir. Vitamin K showed similar patterns with Tecovirimat, with only a few differences (Figure 5D).

As shown in the results various indicators, such as Log P, TPSA, MW, HBA, and HBD must be evaluated for the permeability of drug molecules. Based on Lipinski's rule, these parameters confirmed the viability of the drugs. The review of the literature indicates that drugs approved and available in the market are often administered in different forms. For example, cidofovir is better absorbed through intravenous infusion than oral administration. Cidofovir is rapidly filtered and excreted by the kidney and has a short half-life in cells.[46] The active form of cidofovir, cidofovir diphosphate, is obtained through the phosphorylation of the prodrug by cellular enzymes. Once phosphorylated, the intracellular half-life of cidofovir diphosphate is prolonged.[47] Brincidofovir is a lipid-conjugated analog of cidofovir with better oral absorption. It is hydrolyzed into cidofovir and converted into cidofovir diphosphate by cellular phospholipases, allowing it to pass more effectively through cell membranes, resulting in higher levels of brincidofovir in the cells. Unlike cidofovir, Brincidofovir has less permeability and accumulation in the kidneys, thereby reducing the risk of kidney toxicity.[48] Tecovirimat is formulated for both oral and intravenous administration, with better oral absorption. Co-administration of Brincidofovir and Tecovirimat appears to have a synergistic effect.[49] Based on review studies, vitamin B17 (Amygdalin) is artificially prepared from the natural amygdalin found in the kernels of apricots, peaches, apples, almonds, and cherries and is available for oral and intravenous consumption.[24] However, oral consumption of amygdalin can cause slight poisoning due to the inhibition of cytochrome oxidase in the electron transfer chain in mitochondria. For this reason, it should be consumed only with the advice of a consultant, and it is more appropriate for intravenous injection (the highest dose of amygdalin in the human body is approximately 0.07 g/kg).[50,51] Therefore, it can be argued that while some compounds may not score well for drug-likeness properties, they can still be formulated as drugs by altering their administration form. For instance, they could be administered by injection, topical creams, gels, transdermal patches, suppositories, or nanoliposome drugs, rather than through oral administration.[52] In addition, some traditional techniques such as the use of co-solvents or surfactants, variation of solvent pH, use of hydrates or solvates, inclusion complex formation, or alteration of the dielectric constant of the solvent have been proposed as solutions to improve bioavailability.[53] Thus, it appears that the overall ADMET properties of these compounds reflect their good pharmacokinetic properties, and they may have potential as a drug supplement for the inhibition of the MPox virus.

Conclusion

This study examined the inhibitory effects of various vitamins on the MPox virus and found that vitamins K and

B17 demonstrated good inhibitory effects. In addition, several plant metabolites, such as gingerol in ginger (*Zingiber officinale Roscoe*), rosmarinic acid in selfheal (*Prunella vulgaris L.*), rosemary (*Salvia rosmarinus*), and oregano (*Origanum vulgare*), as well as gallotannin in Aleppo oak (*Quercus infectoria*) and Chinese nutgall (*Rhus chinensis*), were identified as potential inhibitors of the MPox virus. It is important to note that these *in-silico* studies are just the beginning, and further research is necessary to evaluate the clinical effectiveness of these potential inhibitors. In order to better prove the connections and correlations between bioinformatics and experimental studies. It is strongly recommended to conduct more laboratory and clinical research on the plant metabolites and vitamin supplements investigated in this study.

Authors' Contributions

DP and MT have contributed equally to the preparation of the manuscript, with DP collaborating on data collection, content, and data analysis, with the assistance of MT. MT has revised the manuscript, and all authors have approved the final version and are responsible for all aspects of this study.

Conflict of Interest Disclosures

The authors declare that they have no conflicts of interest.

Acknowledgment

The authors express their sincere gratitude to Dr. Mohammad Yaghoubzad at the University of Tabriz for his valuable support in analyzing the molecular dynamic data.

References

1. World Health Organization. WHO recommends new name for monkeypox disease. Available from: https://www.who.int [accessed 28 November 2022]
2. Hoque SF, Bappy MN, Chowdhury AT, Parvez MS, Ahmed F, Imran MA, et al. Scrutinizing surface glycoproteins and poxin-schlafen protein to design a heterologous recombinant vaccine against monkeypox virus. bioRxiv. 2020. doi:10.1101/2020.01.25.919332
3. Henderson DA. The eradication of smallpox–an overview of the past, present, and future. Vaccine. 2011;29:D7-9. doi:10.1016/j.vaccine.2011.06.080
4. McCollum AM, Damon IK. Human monkeypox. Clin Infect Dis. 2014;58(2):260-7. doi:10.1093/cid/cit703
5. World Health Organization. Multi-country monkeypox outbreak in non-endemic countries. In: Disease Outbreak News. [accessed 21 May 2022].
6. Mahase E. Seven monkeypox cases are confirmed in England. BMJ. 2022;377:o1239. doi:10.1136/bmj.o1239
7. Bunge EM, Hoet B, Chen L, Lienert F, Weidenthaler H, Baer LR, et al. The changing epidemiology of human monkeypox—A potential threat? A systematic review. PLOS Negl Trop Dis. 2022;16(2):e0010141. doi:10.1371/journal.pntd.0010141
8. Vaughan A, Aarons E, Astbury J, Brooks T, Chand M, Flegg P, et al. Human-to-human transmission of monkeypox virus, United Kingdom, October 2018. Emerg Infect Dis. 2020;26(4):782-5. doi:10.3201/eid2604.191164
9. Mahase E. Monkeypox: What do we know about the outbreaks in Europe and North America?. BMJ. 2022; 377:o1274. doi:10.1136/bmj.o1274
10. Giorgi FM, Pozzobon D, Di Meglio A, Mercatelli D. Genomic characterization of the recent monkeypox outbreak. Biorxiv. 2022. doi:10.1101/2022.06.01.494368
11. Lam HY, Guan JS, Mu Y. *In silico* repurposed drugs against monkeypox virus. Molecules. 2022;27(16):5277. doi:10.3390/molecules27165277
12. Tesini BL. Monkeypox. 2020. Available from: https://www.msdmanuals.com/en-sg/professional/infectious-diseases/pox-viruses/monkeypox
13. Shchelkunov SN, Totmenin AV, Babkin IV, Safronov PF, Ryazankina OI, Petrov NA, et al. Human monkeypox and smallpox viruses: genomic comparison. FEBS Lett. 2001;509(1):66-70. doi:10.1016/S0014-5793(01)03144-1
14. Musarra-Pizzo M, Pennisi R, Ben-Amor I, Mandalari G, Sciortino MT. Antiviral activity exerted by natural products against human viruses. Viruses. 2021;13(5):828. doi:10.3390/v13050828
15. Barbieri R, Coppo E, Marchese A, Daglia M, Sobarzo-Sánchez E, Nabavi SF, et al. Phytochemicals for human disease: An update on plant-derived compounds antibacterial activity. Microbiol Res. 2017;196:44-68. doi:10.1016/j.micres.2016.12.003
16. Thomford NE, Senthebane DA, Rowe A, Munro D, Seele P, Maroyi A, et al. Natural products for drug discovery in the 21st century: innovations for novel drug discovery. Int J Mol Sci. 2018;19(6):1578. doi:10.3390/ijms19061578
17. Denaro M, Smeriglio A, Barreca D, De Francesco C, Occhiuto C, Milano G, et al. Antiviral activity of plants and their isolated bioactive compounds: An update. Phytother Res. 2020;34(4):742-68. doi:10.1002/ptr.6575
18. Müller B, Kräusslich HG. Antiviral strategies. Handb Exp Pharmacol. 2009;189:1-24. doi:10.1007/978-3-540-79086-0_1
19. Saul AW. Vitamin C Protects Against Coronavirus. Orthomolecular Medicine News Service. 2020.
20. Jayawardena R, Sooriyaarachchi P, Chourdakis M, Jeewandara C, Ranasinghe P. Enhancing immunity in viral infections, with special emphasis on COVID-19: A review. Diabetes Metab Syndr. 2020;14(4):367-82. doi:10.1016/j.dsx.2020.04.015
21. Taheri S, Asadi S, Nilashi M, Abumalloh RA, Ghabban NM, Yusuf SY, et al. A literature review on beneficial role of vitamins and trace elements: Evidence from published clinical studies. J Trace Elem Med Biol. 2021;67:126789. doi:10.1016/j.jtemb.2021.126789
22. Desai AP, Dirajlal-Fargo S, Durieux JC, Tribout H, Labbato D, McComsey GA. Vitamin K & D deficiencies are independently associated with COVID-19 disease severity. Open Forum Infect Dis. 2021;8(10):ofab408. doi:10.1093/ofid/ofab408
23. Lin CC, Liu WH, Wang ZH, Yin MC. Vitamins B status and antioxidative defense in patients with chronic hepatitis B or hepatitis C virus infection. Eur J Nutr. 2011;50:499-506. doi:10.1007/s00394-010-0156-1
24. Saini D, Rawat N, Negi T, Barthwal R, Sharma SK. Utilization, valorization and functional properties of wild apricot kernels. J Pharmacogn Phytochem. 2021;10(4): 119-26.
25. Ioannis P, Anastasis S, Andreas Y. Tripterygium wilfordii extract (Triptolide) and amygdalin promotes cell death in

cancer cells: true or a myth. Am J Cancer Prev. 2015;3(4):77-83. doi:10.12691/ajcp-3-4-3
26. Yildirim FA, Askin MA. Variability of amygdalin content in seeds of sweet and bitter apricot cultivars in Turkey. Afr J Biotechnol. 2010;9(39):6522-4.
27. Kim S, Chen J, Cheng T, Gindulyte A, He J, He S, et al. PubChem 2023 update. Nucleic Acids Res. 2023;51(D1): D1373-80. doi:10.1093/nar/gkac956
28. Wishart DS, Feunang YD, Guo AC, Lo EJ, Marcu A, Grant JR, et al. DrugBank 5.0: a major update to the DrugBank database for 2018. Nucleic Acids Res. 2018;46(D1): D1074-82. doi:10.1093/nar/gkx1037
29. Gao A, Gao S. In silico identification of non-cross-reactive epitopes for monkeypox cell surface-binding protein. Research Square. 2022. doi:10.21203/rs.3.rs-1693979/v1
30. Yang J, Yan R, Roy A, Xu D, Poisson J, Zhang Y. The I-TASSER Suite: protein structure and function prediction. Nat Methods. 2015;12(1):7-8. doi:10.1038/nmeth.3213
31. Heble NK, Mavillapalli RC, Selvaraj R, Jeyabalan S. Molecular docking studies of phytoconstituents identified in Crocus sativus, Curcuma longa, Cassia occidentalis and Moringa oleifera on thymidylate synthase–an enzyme target for anti-cancer activity. J Appl Pharm Sci. 2016;6(12):131-5. doi:10.7324/JAPS.2016.601218
32. Manavi MA. *In silico* Study to Identification of Potential SARS-CoV-2 Main Protease Inhibitors: Virtual Drug Screening and Molecular Docking with AutoDock Vina and Molegro Virtual Docker. J Cell Mol Res. 2022;13(2): 108-12. doi:10.22067/jcmr.2021.71517.1013
33. Ibrahim ZY, Uzairu A, Shallangwa G, Abechi S. Molecular docking studies, drug-likeness and in-silico ADMET prediction of some novel β-Amino alcohol grafted 1, 4, 5-trisubstituted 1, 2, 3-triazoles derivatives as elevators of p53 protein levels. Sci Afr. 2020;10: e00570. doi:10.1016/j.sciaf.2020.e00570
34. Nelson MT, Humphrey W, Gursoy A, Dalke A, Kalé LV, Skeel RD, et al. NAMD: a parallel, object-oriented molecular dynamics program. Int J High Perform Comput Appl. 1996;10(4):251-68. doi:10.1177/10943420961000401
35. Humphrey W, Dalke A, Schulten K. VMD: visual molecular dynamics. J Mol Graph. 1996;14(1):33-8. doi:10.1016/0263-7855(96)00018-5
36. Lopes PE, Huang J, Shim J, Luo Y, Li H, Roux B, et al. Polarizable force field for peptides and proteins based on the classical drude oscillator. J Chem Theory Comput. 2013;9(12):5430-49. doi:10.1021/ct400781b
37. Pradeepkiran JA, Kumar KK, Kumar YN, Bhaskar M. Modeling, molecular dynamics, and docking assessment of transcription factor rho: a potential drug target in *Brucella melitensis* 16M. Drug Des Devel Ther. 2015:1897-912.
38. Zoete V, Cuendet MA, Grosdidier A, Michielin O. SwissParam: a fast force field generation tool for small organic molecules. J Comput Chem. 2011;32(11):2359-68. doi:10.1002/jcc.21816
39. Bishop TC, Kosztin D, Schulten K. How hormone receptor-DNA binding affects nucleosomal DNA: the role of symmetry. Biophys J. 1997;72(5):2056-67. doi:10.1016/S0006-3495(97)78849-0
40. Ibrahim MT, Uzairu A, Shallangwa GA, Uba S. Molecular docking investigation and pharmacokinetic properties prediction of some anilinopyrimidines analogues as egfr t790m tyrosine kinase inhibitors. Egypt J Basic Appl Sci. 2021;8(1):203-13. doi:10.1080/2314808X.2021.1946650
41. Hadni H, Elhallaoui M. 3D-QSAR, docking and ADMET properties of aurone analogues as antimalarial agents. Heliyon. 2020;6(4):e03580. doi:10.1016/j.heliyon.2020.e03580
42. Holford N, Yim DS. Clearance. Transl Clin Pharmacol. 2015;23(2):42-5. doi:10.12793/tcp.2015.23.2.42
43. Hutson CL, Kondas AV, Mauldin MR, Doty JB, Grossi IM, Morgan CN, et al. Pharmacokinetics and efficacy of a potential smallpox therapeutic, brincidofovir, in a lethal monkeypox virus animal model. MSphere. 2021;6(1):10-128. doi:10.1128/msphere.00927-20
44. Matias WR, Koshy JM, Nagami EH, Kovac V, Moeng LR, Shenoy ES, et al. Tecovirimat for the treatment of human monkeypox: an initial series from Massachusetts, United States. Open Forum Infect Dis. 2022;9(8):ofac377. doi:10.1093/ofid/ofac377
45. Siegrist EA, Sassine J. Antivirals with activity against mpox: a clinically oriented review. Clin Infect Dis. 2023;76(1):155-64. doi:10.1093/cid/ciac622
46. Yu J, Raj SM. Efficacy of three key antiviral drugs used to treat orthopoxvirus infections: a systematic review. Global Biosecurity. 2019;1(1):28-74.
47. Magee WC, Hostetler KY, Evans DH. Mechanism of inhibition of vaccinia virus DNA polymerase by cidofovir diphosphate. Antimicrob Agents Chemother. 2005;49(8): 3153-62. doi:10.1128/aac.49.8.3153-3162.2005
48. Painter W, Robertson A, Trost LC, Godkin S, Lampert B, Painter G. First pharmacokinetic and safety study in humans of the novel lipid antiviral conjugate CMX001, a broad-spectrum oral drug active against double-stranded DNA viruses. Antimicrob Agents Chemother. 2012;56(5):2726-34. doi:10.1128/aac.05983-11
49. Jordan R, Chinsangaram J, Bolken TC, Tyavanagimatt SR, Tien D, Jones KF, et al. Safety and pharmacokinetics of the antiorthopoxvirus compound ST-246 following repeat oral dosing in healthy adult subjects. Antimicrob Agents Chemother. 2010;54(6):2560-6. doi:10.1128/aac.01689-09
50. Jaswal V, Palanivelu J, Ramalingam C. Effects of the Gut microbiota on Amygdalin and its use as an anti-cancer therapy: Substantial review on the key components involved in altering dose efficacy and toxicity. Biochem Biophys Rep. 2018;14:125-32. doi:10.1016/j.bbrep.2018.04.008
51. Song Z, Xu X. Advanced research on anti-tumor effects of amygdalin. J Cancer Ther. 2014;10(Suppl 1):C3-7. doi:10.4103/0973-1482.139743
52. Gomez-Orellana I. Strategies to improve oral drug bioavailability. Expert Opin Drug Deliv. 2005;2(3):419-33. doi:10.1517/17425247.2.3.419
53. Kansara H, Panola R, Mishra A. Techniques used to enhance bioavailability of BCS class II drugs: a review. Int J Drug Dev Res. 2015;7(1):82-93.